J|A|C|S COMMUNICATIONS

Published on Web 05/27/2010

Measurement of Site-Specific ^{13}C Spin−Lattice Relaxation in a Crystalline Protein

Józef R. Lewandowski,[†] Julien Sein,[†] Hans Jürgen Sass,[§] Stephan Grzesiek,[§] Martin Blackledge,[‡] and Lyndon Emsley*,[†]

Université de Lyon, CNRS/ENS-Lyon/UCB-Lyon 1, Centre de RMN à Très Hauts Champs, 69100 Villeurbanne, France, Protein Dynamics and Flexibility, Institut de Biologie Structurale Jean Pierre Ebel, UMR 5075, CNRS/CEA/UJF, 38027 Grenoble, France, and Biozentrum, Universität Basel, 4056 Basel, Switzerland

Received April 1, 2010; E-mail: lyndon.emsley@ens-lyon.fr

Understanding the chemical processes of life depends crucially on the development of an atomic resolution description of protein structure and dynamics. Furthermore, molecular motion is at the core of enzymatic catalysis, molecular recognition, signaling, ligand binding, and protein folding.[1] Today, NMR is the best available method for probing site-specific biomolecular motions, both in solution and in the solid state. However, in the solid state the key barrier to discriminating between different models for protein dynamics (e.g., Anisotropic Collective Motions[2] vs completely uncorrelated local motions) is the scarcity of observables. Indeed the only parameter currently providing both a time scale and an amplitude of motion in uniformly ^{13}C, ^{15}N labeled biopolymers is ^{15}N spin−lattice (R_1) relaxation.[3] However, even with multiple-field measurements, the information is too sparse to unambiguously describe complex motions.[4] For comparison, in solution, over 20 measurements can be made per residue in state-of-the-art solution studies, providing quantitative characterization of backbone motions occurring on time scales up to the millisecond.[5] Consequently, to provide a more comprehensive picture of biomolecular motions in solids, development of new probes is required.

Previously it has not been possible to measure ^{13}C spin−lattice relaxation rates in a site-specific manner because in labeled proteins rapid proton driven carbon−carbon spin diffusion (PDSD) homogenizes the rates over all sites.[6,7] Here we demonstrate the measurement of site-specific backbone and side-chain ^{13}C spin−lattice relaxation rates in a uniformly ^{13}C labeled nanocrystalline protein using ultrafast magic angle spinning to overcome the spin diffusion problem.

The influence of PDSD on the measured R_1 rates is notably more complicated for ^{13}C spins than ^{15}N spins. ^{15}N has a lower γ and is more sparsely distributed than ^{13}C, so that averaging of the ^{15}N rates by PDSD only concerns sequential backbone nitrogens, separated from each other by three bonds.[6] At sample spinning frequencies above 10 kHz, ^{15}N PDSD is slow enough compared to the relaxation rates to have only a small effect on site-specific R_1 measurements.[6]

The case of ^{13}C is fundamentally different because PDSD is much more efficient within the dense network of directly bonded carbons. At a sample spinning frequency of 16 kHz, the effect of PDSD is not just a correction factor; it dominates the measurement of R_1's, as is demonstrated by the values measured for [U-^{13}C,^{15}N]-Ala given in Table 1.

We have found that by increasing the spinning frequency to 60 kHz, achievable using 1.3 mm rotors in state-of-the-art NMR probes, PDSD rates are reduced to the extent that they become much smaller than the R_1's. We show in the following that this allows reliable measurement of site-specific R_1's in the protein GB1. To demonstrate this principle we performed test experiments on "dry" crystalline [U-^{13}C,^{15}N]-Ala and [U-^{13}C,^{15}N]-Ile. Table 1 lists the decay rates of the longitudinal magnetization in [U-^{13}C,^{15}N]-Ala measured at $\omega_r/2\pi = 16.1$ and 60.0 kHz (for similar data for [U-^{13}C,^{15}N]-Ile, see Supporting Information (SI)). We see that at $\omega_r/2\pi = 16.1$ kHz the decay rates for the three sites are quite similar (dominated by the methyl relaxation). However, the situation is radically different at $\omega_r/2\pi = 60$ kHz *where we observe order of magnitude differences in the measured rates between sites*. To determine how close the measured rates are to the actual site-specific R_1's, we performed analogous measurements on [1-^{13}C]-Ala and [2-^{13}C]-Ala in which the influence of intramolecular PDSD is eliminated. Figure 1a shows the relaxation profiles for the C′ site in [1-^{13}C]-Ala and [U-^{13}C,^{15}N]-Ala at a spinning frequency of 60 kHz. Due to both the large chemical shift difference between C′ and the aliphatic carbons and the high spinning frequency, the PDSD rate is slowed down to the extent that we record almost identical curves (maximum intensity difference ∼3%) for C′ in both samples with measured rates of 0.032 and 0.030 s^{-1} respectively (we remark that the difference of 0.002 s^{-1} is ∼12 times less than the average experimental error for C′ in GB1).

Table 1. ^{13}C Longitudinal Magnetization Decay Rates for [U-^{13}C,^{15}N]-Ala Measured at $\omega_r/2\pi = 16.1$ and 60.0 kHz[a]

[U-^{13}C,^{15}N]-Ala Site	$\omega_r/2\pi = 16.1$ kHz Measured Rate (s^{-1})	$\omega_r/2\pi = 60$ kHz Measured Rate (s^{-1})
C′	1.484 ± 0.013	0.031 ± 7e-5
C_α	1.579 ± 0.009	0.205 ± 0.002
$C_\beta(CH_3)$	2.492 ± 0.141	12.076 ± 0.060

[a] The measurements were performed at ambient temperature with $\omega_{H0}/2\pi = 900$ MHz.

Moreover, the measurement at the Cα site (Figure 1b) also yields quite similar rates for [U-^{13}C,^{15}N] and [2-^{13}C] labeled samples (0.21 and 0.16 s^{-1} respectively). This suggests that the measurements for the aliphatic sites in fully labeled Ala also yield rates that are close to the actual ^{13}C R_1′s (even though, compared to the C′ case, they are characterized by a slightly larger deviation of the apparent rate from the true site-specific value due to some residual PDSD averaging). We remark that in general the deviation of the measured rate from the true site-specific R_1 will be largest for ^{13}C nuclei having a directly bonded neighbor with a small chemical shift separation (see SI).

Note that the difference between the two alanine Cα measurements above ($\Delta R_1 \sim 0.05$ s^{-1}) is on the order of the present average experimental error in the data recorded on protein samples (the

[†] Université de Lyon.
[‡] Institut de Biologie Structurale Jean Pierre Ebel,.
[§] Universität Basel.

10.1021/ja102744b

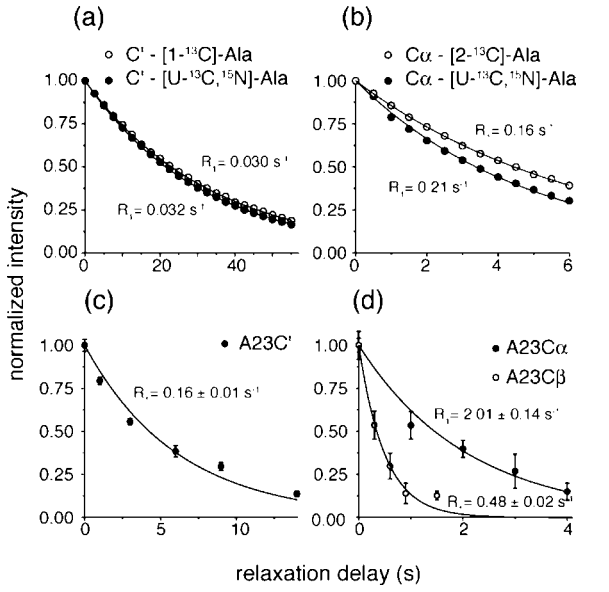

Figure 1. ^{13}C longitudinal magnetization decay curves in crystalline alanine (a−b) and A23 of [U-^{13}C,^{15}N]-GB1 (c−d). (a) C′ in [U-^{13}C,^{15}N]-Ala and [1-^{13}C]-Ala (Yielding measured R_1 of 0.0323 ± (7.3 × 10^{-5}) and 0.0302 ± (5.4 × 10^{-5}) s^{-1} respectively). (b) Cα in [U−^{13}C,^{15}N]-Ala and [2-^{13}C]-Ala (Yielding measured R_1 of 0.205 ± 0.002 and 0.156 ± (4.8 × 10^{-4}) s^{-1} respectively). The experiments in (a−b) were performed at $\omega_r/2\pi = 60$ kHz, $\omega_{H0}/2\pi = 900$ MHz, and ambient temperature. The experiments in (c−d) were performed at $\omega_r/2\pi = 60$ kHz, $\omega_{H0}/2\pi = 800$ MHz, and 278 ± 2 K. The error bars in (c−d) reflect twice the standard deviation of the spectral noise.

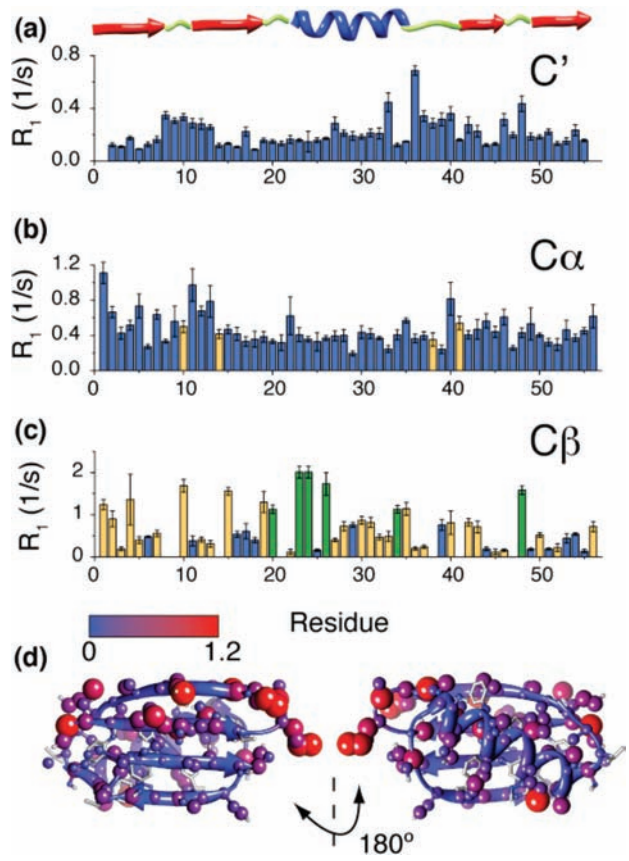

Figure 2. C′ (a), Cα (b), and Cβ (c) spin−lattice relaxation rates measured for [U-^{13}C,^{15}N]-GB1. Blue bars indicate CH, yellow CH_2, and green CH_3 groups. (d) Mapping of side-chain ^{13}C R_1 normalized to the number of directly attached ^{1}H onto the GB1 structure (PDB 2gi9[22]); the rates are indicated with both color and ball radius. The rates were measured with $\omega_r/2\pi = 60$ kHz and $\omega_{0H}/2\pi = 800$ MHz at 278 ± 2 K.

average error in GB1 (below) for Cα′s is 0.07 s^{-1}). In addition, since hydrated proteins are generally more dynamic than single crystalline amino acids, they have larger relaxation rates (see Figure 1). This, combined with the fact that PDSD (which is a coherent process) should be quite similar in both types of sample, means that the deviations of measured rates from the site-specific R_1's due to PDSD averaging should be even smaller in a protein than in alanine. We therefore conclude that under 60 kHz MAS we should be able to measure carbon-13 C′ and Cα (and possibly side-chain) R_1's in a site-specific manner with negligible or small deviations.

C′ and Cα spin−lattice rates were recorded for microcrystalline [U-^{13}C,^{15}N]-GB1 using NCO and NCA type experiments.[8] Side-chain spin−lattice relaxation rates were recorded in a ^{13}C−^{13}C 2D correlation experiment with selective aliphatic CP[9] and RFDR[10] mixing. The measured rates are listed in Table SI2. During t_1 evolution and acquisition we applied heteronuclear decoupling using a new scheme that we refer to as swept low power TPPM (slpTPPM). The sweep[11] through the low power TPPM condition[12] was achieved by varying linearly the duration of the TPPM pulses (in a manner similar to SW_f-TPPM[13]) with each of the pulse lengths in the middle of the decoupling cycle equal to two rotor periods each (see SI). slpTPPM achieves decoupling over a greater bandwidth when compared to the unmodified low power TPPM and yields favorable T_2' (see SI). In addition to R_1 measurements we performed a number of control PDSD experiments. The 6 s PDSD spectrum (Figure SI4) acquired with initial magnetization on C′ is devoid of cross peaks. This confirms that at $\omega_r/2\pi = 60$ kHz and $\omega_{H0}/2\pi = 800$ MHz the effect of intraresidue PDSD on C′ rates is safely negligible. However, NCO experiments indicate that there is occasionally residual PDSD transfer between sequential C′ sites with $\Delta\delta_{cs} < 1.5$ ppm. For other ^{13}C spins the control 2 s aliphatic PDSD spectrum (Figure SI3) shows a number of cross peaks for directly bonded carbons with small chemical shift differences, as well as for a few sequential Cα peaks.[13]

These control spectra allow us to evaluate approximate PDSD rates. Using an exchange model[10] we have estimated (details given in SI) that the maximum difference induced by inter-residue PDSD averaging between the measured rates and the actual R_1's should be on the order of or less than the experimental error. The deviations of the measured rates from the site-specific R_1's are thus in general small, and while they should be taken into account in quantitative analysis (most simply by appropriately increasing the error bars) they are sufficiently small to allow for site-specific analysis of backbone and side-chain dynamics in biopolymers. Note that measured deviations from the true site-specific rates should be further reduced if higher spinning frequencies and/or higher magnetic fields are employed and/or in more sparsely labeled samples.

Figure 2 shows the measured C′, Cα, and side-chain spin−lattice relaxation rates for GB1. Notably, we observe large (up to 6-fold) variations in rates over the primary sequence. To further validate the measurements, we note interesting correlations between measured rates and known dynamical features of GB1 (or closely related GB3) when the rates are mapped onto the structure of the protein, as illustrated in Figure 3. In particular Figure 3 shows that C′ R_1's are well matched across different strands with faster rates on the edges of the sheet and slower rates in the center. C′ rates are weakly correlated with residue solvent accessibility[15] (Pearson correlation coefficient 0.31 with a significance level of 0.05, as can be appreciated visually in Figure 3d). The rates could also be

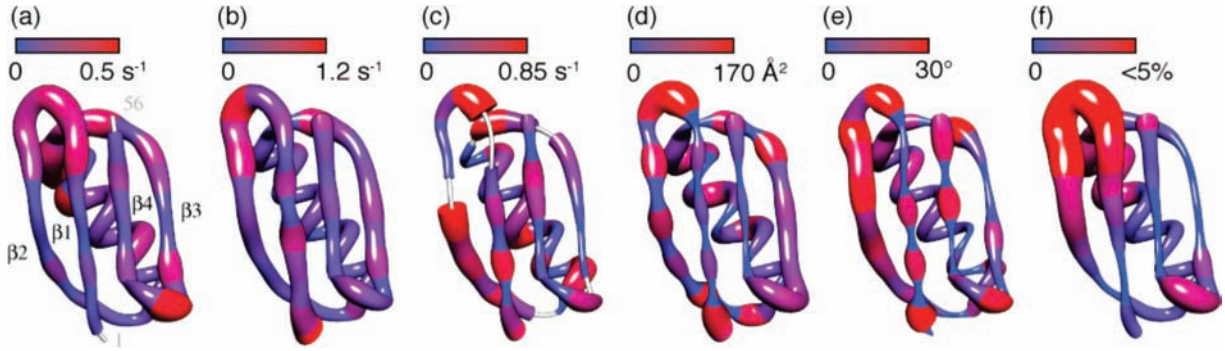

Figure 3. GB1 R_1 rates (C′ in (a), Cα in (b), and Cβ normalized to the number of attached protons in (c)) vs (d) residue solvent accessibility[15] in GB1, (e) 3D GAF γ fluctuations determined for GB3 from RDCs in solution,[16] and (f) contributions to the lowest eigenmode of the PCA analysis of AMD of GB3.[17] The magnitude of all of the properties is indicated both by the color and by the radius of the "worm" projected onto the GB1 structure (PDB ID 2gi9[14]).

suggestive of collective motions of the β-sheet. A similar alternating pattern of rates is observed in the case of the Cα sites in the β-sheet involving the same peptide planes. Moreover, Cα rates exhibit periodic modulation in the helix (which corresponds to slower R_1's on one side of the helix and faster on the other side; a similar pattern was recently observed for Dα R_{1Z} rates in solution[18]). The combined distribution of measured rates suggests the largest amount of dynamics is in loop I followed by the C-terminal part of the helix, loop IV, and the external β_2 strand, a pattern resembling the patterns determined for GB3 (which is highly analogous to GB1) both from 3D GAF analysis of RDCs in solution[16] (see Figure 3e) and Accelerated Molecular Dynamics (see Figure 3f).[17]

In summary, we have shown that proton driven carbon−carbon spin diffusion, which previously lead to averaging of carbon-13 spin−lattice relaxation rates under all experimentally accessible conditions in labeled proteins, can be reduced to an almost insignificant contribution by ultrafast (>60 kHz) magic angle spinning. This has allowed us to measure site-specific C′, Cα, and side-chain carbon longitudinal relaxation rates in the protein GB1 and so provides a new probe of fast (ps−ns) time scale dynamics of solid proteins without the need for deuteration or specific labeling (even though such labeling may be considered to further reduce the extent of PDSD averaging in the future). A combination of ^{13}C and ^{15}N spin−lattice relaxation and RDC measurements[19] should allow for more comprehensive descriptions of motions in biopolymers and so allow for the discrimination between different physical models of motion, including e.g. Anisotropic Collective Motions.[2]

Acknowledgment. We would like to thank Nicolas Giraud for helpful discussions. This work was supported in part by the Agence Nationale de la Recherche (ANR PCV 2007 Protein Motion) and the Access to Research Infrastructures activity in the 6th Framework Program of the EC (RII3-026145, EU-NMR). J.R.L. was supported by EU IRG (PIRG03-GA-2008-231026). Molecular graphics images were produced with Chimera, UCSF.[20]

Supporting Information Available: Measured rates for [U-^{13}C,^{15}N]-Ile. Control PDSD spectra. Table of ^{13}C spin−lattice rates measured on [U-^{13}C,^{15}N]-GB1 (including backbone and side chains). Tables of PDSD induced cross peaks and approximate PDSD rates. Experimental details including slpTPPM setup. This material is available free of charge via the Internet at http://pubs.acs.org.

References

(1) Boehr, D. D.; Dyson, H. J.; Wright, P. E. *Chem. Rev.* **2006**, *106*, 3055–3079.
(2) Lewandowski, J. R.; Sein, J.; Blackledge, M.; Emsley, L. *J. Am. Chem. Soc.* **2009**, *132*, 1245–8.
(3) (a) Giraud, N.; Blackledge, M.; Goldman, M.; Böckmann, A.; Lesage, A.; Penin, F.; Emsley, L. *J. Am. Chem. Soc.* **2005**, *127*, 18190–18201. (b) Chevelkov, V.; Diehl, A.; Reif, B. *J. Chem. Phys.* **2008**, *128*, 052316.
(4) Wang, T. Z.; Cai, S.; Zuiderweg, E. R. P. *J. Am. Chem. Soc.* **2003**, *125*, 8639–8643.
(5) (a) Lakomek, N. A.; Walter, K. F. A.; Fares, C.; Lange, O. F.; de Groot, B. L.; Grubmuller, H.; Bruschweiler, R.; Munk, A.; Becker, S.; Meiler, J.; Griesinger, C. *J. Biomol. NMR* **2008**, *41*, 139–155. (b) Markwick, P. R. L.; Bouvignies, G.; Salmon, L.; McCammon, J. A.; Nilges, M.; Blackledge, M. *J. Am. Chem. Soc.* **2009**, *131*, 16968–16975. (c) Palmer, A. G. *Chem. Rev.* **2004**, *104*, 3623–3640. (d) Salmon, L.; Bouvignies, G.; Markwick, P.; Lakomek, N.; Showalter, S.; Li, D. W.; Walter, K.; Griesinger, C.; Brüschweiler, R.; Blackledge, M. *Angew. Chem., Int. Ed.* **2009**, *48*, 4154–4157.
(6) Giraud, N.; Blackledge, M.; Bockmann, A.; Emsley, L. *J. Magn. Reson.* **2007**, *184*, 51–61.
(7) Krushelnitsky, A.; Brauniger, T.; Reichert, D. *J. Magn. Reson.* **2006**, *182*, 339–342.
(8) Giraud, N.; Böckmann, A.; Lesage, A.; Penin, F.; Blackledge, M.; Emsley, L. *J. Am. Chem. Soc.* **2004**, *126*, 11422–11423.
(9) Laage, S.; Marchetti, A.; Sein, J.; Pierattelli, R.; Sass, H. J.; Grzesiek, S.; Lesage, A.; Pintacuda, G.; Emsley, L. *J. Am. Chem. Soc.* **2008**, *130*, 17216–17.
(10) Bennett, A. E.; Ok, J. H.; Griffin, R. G.; Vega, S. *J. Chem. Phys.* **1992**, *96*, 8624–8627.
(11) (a) Verel, R.; Ernst, M.; Meier, B. H. *J. Magn. Reson.* **2001**, *150*, 81–99. (b) De Paëpe, G.; Bayro, M. J.; Lewandowski, J.; Griffin, R. G. *J. Am. Chem. Soc.* **2006**, *128*, 1776–1777.
(12) (a) De Paëpe, G. Heteronuclear Decoupling in SSNMR, Doctoral Thesis, Ecole Normale Supérieure de Lyon, 2004. (b) Kotecha, M.; Wickramasinghe, N. P.; Ishii, Y. *Magn. Reson. Chem.* **2007**, *45*, S221–S230.
(13) (a) Thakur, R. S.; Kurur, N. D.; Madhu, P. K. *Chem. Phys. Lett.* **2006**, *426*, 459–463. (b) Chandran, C. V.; Madhu, P. K.; Kurur, N. D.; Brauniger, T. *Magn. Reson. Chem.* **2008**, *46*, 943–947. Our observation of a rapid drop in PDSD rates between carbons with large chemical shift differences with increasing ω_r is in line with recent observations in small molecules by Ernst M. et al. - private communication.
(14) Franks, W. T.; Wylie, B. J.; Stellfox, S. A.; Rienstra, C. M. *J. Am. Chem. Soc.* **2006**, *128*, 3154–3155.
(15) Gerstein, M. *Acta Crystallogr., Sect. A* **1992**, *48*, 271–276.
(16) Bouvignies, G.; Bernado, P.; Meier, S.; Cho, K.; Grzesiek, S.; Brüschweiler, R.; Blackledge, M. *Proc. Natl. Acad. Sci. U.S.A.* **2005**, *102*, 13885–13890.
(17) Markwick, P. R. L.; Bouvignies, G.; Blackledge, M. *J. Am. Chem. Soc.* **2007**, *129*, 4724–4730.
(18) Sheppard, D.; Li, D. W.; Brüschweiler, R.; Tugarinov, V. *J. Am. Chem. Soc.* **2009**, *131*, 15853–15865.
(19) Lorieau, J. L.; McDermott, A. E. *J. Am. Chem. Soc.* **2006**, *128*, 11505–11512.
(20) Pettersen, E. F.; Goddard, T. D.; Huang, C. C.; Couch, G. S.; Greenblatt, D. M.; Meng, E. C.; Ferrin, T. E. *J. Comput. Chem.* **2004**, *25*, 1605–1612.

JA102744B